Progress in Organic Coatings 88 (2015) 8–16

Contents lists available at ScienceDirect

Progress in Organic Coatings

journal homepage: www.elsevier.com/locate/porgcoat

Waterborne acrylic–casein latexes as eco-friendly binders for coatings

Matías L. Picchio[a,b], Mario C.G. Passeggi Jr.[c], María J. Barandiaran[d], Luis M. Gugliotta[a], Roque J. Minari[a,*]

[a] Group of Polymers and Polymerization Reactors, INTEC (Universidad Nacional del Litoral-CONICET), Güemes 3450, Santa Fe 3000, Argentina
[b] Facultad Regional Villa María (Universidad Tecnológica Nacional), Av. Universidad 450, Villa María 5900, Argentina
[c] Physics of Surfaces and Interfaces Laboratory, IFIS Litoral (Universidad Nacional del Litoral-CONICET), Güemes 3450, Santa Fe 3000, Argentina
[d] POLYMAT and Departamento de Química Aplicada, University of the Basque Country UPV/EHU, Centro Joxe Mari Korta, Avenida Tolosa 72, 20018, Donostia-San Sebastián, Spain

ARTICLE INFO

Article history:
Received 27 February 2015
Received in revised form 23 May 2015
Accepted 10 June 2015

Keywords:
Hybrid nanoparticles
Casein–acrylic
Biodegradable coatings

ABSTRACT

The use of casein as renewable resource to produce eco-friendly hybrid latexes has an increasing importance in industrial applications especially for high performance waterborne coatings. This work describes the synthesis of hybrid acrylic–casein latexes by emulsion polymerization of acrylic monomers in presence of varied casein concentration, and in absence of emulsifier which is usually a challenge for preparing stable nanocomposite latexes. The production and microstructure characterization of the casein–acrylic nanoparticles, as well as the properties of the films obtained from the hybrid latexes are here reported. The synthesized acrylic–casein latexes are able to form films with promising properties for a potential application as waterborne bio-based coatings.

1. Introduction

In recent years, considerable efforts have been made by the polymer industry to develop environmentally benign processes that avoid the emission of volatile organic compounds (VOC) and to substitute petroleum based monomers by renewable raw materials. In the coatings field, waterborne dispersed polymers used as binders, appear as an environmentally friendly alternative to solvent-based coatings [1]. Also, proteins have a large potential for the substitution of currently used petrochemicals, since monomers and polymers can be derived from these resources [2]. Indeed, casein derived from bovine milk, is a very practicable biomaterial with good biocompatibility and biodegradability, easily available at high purity and low cost [3]. Casein had long been used in film formation applications, as principal binder in leather finishing, paper coating and adhesive, due to its good stained acceptance, finishing glazed aspect, good substrate penetrability and strong adhesive force [4,5]. However, the casein films are highly susceptible to microbial attack, to wet rub and present low flexibility and extensibility [6].

One of the biggest challenges for binders employed in waterborne coatings is to simultaneously attain two contradictory requirements: (a) a low minimum film formation temperature (MFFT < 15 °C), to ensure a smooth film formation under applications at room temperature; and (b) acceptable blocking resistance and film hardness, which is usually accomplished by polymers with a T_g above the room temperature. Traditionally, coalescing agents are used to plasticize the binder during film formation, decreasing its T_g and allowing the formation of a smooth film at room temperature. Once the film is formed, the coalescent evaporates and the film may recover its hardness and blocking characteristics. However, in addition to the environmental problem of releasing VOCs to atmosphere, the marketplace is also demanding coatings with less odor, and the coalescing solvents in a latex paint are clearly one source of odor. Other alternative to solve this issue is to introduce a harder phase to a soft binder that will bloom to the top of a film as it dries. Typically, solutions involve the use of blends of hard/soft latex particles [7–16] or surface-active agents as silicon-based materials, waxes and/or fluorinated additives. In this scenery, the use of a natural compound with a high T_g (~180 °C), as casein, in combination with a soft acrylic polymer appears as a promising system to produce waterborne nanostructured binders that simultaneously attain these antagonistic requirements.

Emulsion polymerization of acrylic monomers in the presence of casein has been previously studied in aqueous media using persulfate initiators and in absence of emulsifier [17–21], due to the marked amphiphilic character of casein that makes it an important surface-active agent [22]. In such works [17–21], the

* Corresponding author. Tel.: +54 3424559174; fax: +54 3424511079.
E-mail address: rjminari@santafe-conicet.gov.ar (R.J. Minari).

http://dx.doi.org/10.1016/j.porgcoat.2015.06.012
0300-9440/

effect of concentrations of initiator, monomer and casein on the grafting extent, was studied. Also, casein-based latexes as film-forming materials were previously synthesized by utilizing persulfate initiators together with sodium hydrogensulfite as a redox pair [23,24]. However, casein is easily oxidized in the presence of these initiators, producing yellowish coatings which are undesirable from the esthetic point of view [3]. Recently, a crosslinkable acrylic resin/protein composite emulsion was obtained by mixing a latex containing ketone carbonyl groups with a certain amount of gelatin or casein, which act as a crosslinking agent [25]. Composite films with improved hardness, tensile strength, and water and solvent resistance were obtained.

Li et al. also reported the synthesis of casein–poly(methyl methacrylate) (PMMA) nanoparticles via emulsifier-free emulsion polymerization [26,27]. Grafting of casein with PMMA was conducted by initiating the polymerization according to a redox reaction between an alkyl hydroperoxide and the amino groups of the casein. Then, the propagation of amino casein radicals produces the protein graft polymerization and the formation of compatibilized nanoparticles. In a recent work [28], we quantified the grafting degree of casein along the MMA emulsion polymerization performed in the presence of varied casein concentration. We observed that as the concentration of casein increased from 3 parts per hundred monomer (pphm) to 25 pphm, the amount of incorporated casein increased, and the situation was opposite up to 50 pphm, the maximum range studied. As a result, two kinds of particles were obtained: the compatibilized ones mainly formed by PMMA-graft-casein and the other ones containing only PMMA homopolymer. However, due to the high T_g of both the bio- and synthetic components, this hybrid system is not valuable for coating formulations.

In this work, the performance of hybrid acrylic–casein latexes as potential binders for coatings was investigated. Firstly, the synthesis of waterborne nanoparticles with different monomer ratios, butyl acrylate (BA)/methyl methacrylate (MMA), and casein concentrations is presented. The redox initiation system proposed by Li et al. [26], which involves tert-butyl hydroperoxide (TBHP) and the casein amines, was here adopted. Next, film properties were analyzed, including film morphology, opacity, MFFT, hardness, blocking, and elongation. Finally, the film biodegradability in composting conditions was evaluated.

2. Materials and methods

2.1. Materials

Technical grade casein from bovine milk (Sigma), MMA and BA monomers containing traces of mono methyl ether hydroquinone as inhibitor (Aldrich) were used. The employed initiator was TBHP (Aldrich). Other used reagents were: sodium carbonate (Na_2CO_3, Cicarelli) as buffer to regulate the pH, methyl ethyl ketone (MEK, Anedra), benzene (Bz, AnalytiCals) and sodium dodecyl sulfate (SDS, Anedra). All the reagents were used as received without purification. Distilled and deionized water was used throughout the work.

2.2. Polymerization process

Polymerizations of BA/MMA in the presence of variable amount of casein were carried out in a 0.5 L glass jacketed reactor equipped with thermostatic bath, digital thermometer, condenser, stirrer, N_2 inlet and sampling device. The BA/MMA ratio was varied from pure BA to 63/37 wt/wt as follows: 100/0, 80/20, 70/30, 65/35 and 63/37. The casein//BA/MMA ratio was adopted as to get a constant theoretical T_g in the range of (−10 °C) for the resulting nanoparticles. In addition, a BA/MMA copolymer (60/40) without casein, which has an estimated T_g of (−10 °C) was also synthesized for comparison purposes. Polymerizations were carried out as follows. Casein was first dissolved in the reactor, in a water solution containing 2.5 pphm of Na_2CO_3 (pH 11) and at 50 °C. At pH higher than 10, maximum casein solubility is reached and a looser micelle structure is obtained due to a reduction in the association of molecules by hydrophobic interaction [29]. Then, the solution temperature was raised up to 80 °C and monomers were loaded. The resulting dispersion was purged with N_2 for 30 min before injecting the TBHP. Polymerizations were run for 300 min with continuous bubbling of N_2 and samples were withdrawn along the process at regular time intervals. Table 1 presents a general recipe of the performed polymerizations.

Table 1
General recipe for the synthesis of poly(BA-co-MMA)–casein hybrid latexes.

Reagent	Amounts (pphm)[a]
BA + MMA	100
Casein	3–50
TBHP	0.20
Na_2CO_3	2.5
H_2O	600

[a] pphm: parts per hundred monomer.

2.3. Latex characterization

The overall monomer conversion (x) was determined gravimetrically and it was defined as the weight ratio between the acrylic polymer and the total amount of acrylic monomers in the formulation (casein was not considered in the x calculation).

Average particle diameters (dp) were measured at 30 °C by dynamic light scattering, using a Brookhaven BI-9000 AT photometer at a detection angle of 90°. Samples were prepared by diluting a fraction of the latex in deionized water, in order to obtain count rates between 100 and 300 kcounts per second. Particle size distribution (PSD) was determined by capillary hydrodynamic fractionation employing a CHDF2000 (Matec Applied Sciences) equipment. Samples were diluted in deionized water to 1.5% of solids content.

The fraction of casein grafted to the acrylic polymer (casein grafting efficiency, CGE) was determined by correlating the mass of grafted casein to the loaded protein. A procedure of multiple centrifugation and redispersion was applied to separate the ungrafted casein from the latex, obtaining the mass of grafted casein from the difference between the loaded and the non-linked casein [28].

2.4. Film characterization

The polymer films were prepared by casting the latexes onto silicone molds and then they were dried at 22 °C and 55% relative humidity during 7 days to assure a constant weight of the film. The polymer films were carefully peeled from the silicone substrate, obtaining a film with a final thickness of about 1 mm.

The morphology and nanomechanical properties of the films were determined by using a commercial Nanotec Electronic Atomic Force Microscope (AFM) operating in tapping and jumping modes, respectively. All the AFM experiments were performed in air at room temperature. Acquisition and image processing were performed using the WS×M free software [30]. Rotated monolitic Budget Sensors All-In-One-Al cantilevers (Budget Sensors, Sofia, Bulgaria) made of silicon with a 30 nm thick aluminum reflex coating and a tip radius <10 nm were used. While the nominal resonance frequency and spring constant of the cantilever used in tapping mode were 350 kHz and 40 N/m, in jumping mode were 80 kHz and 2.7 N/m. Cross-sectionals were obtained by (cryo)microtomy (Leica EM UC6). The root mean squared (RMS) of the roughness of each

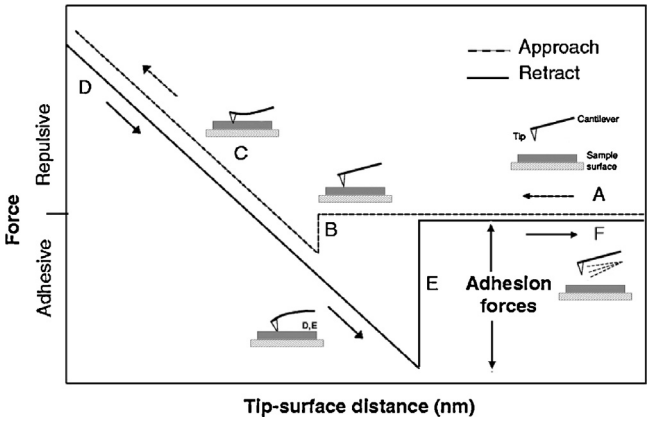

Fig. 1. Sketch of the stages of AFM jumping experiment. Tip/surface contact and cantilever bending with tip indentation occur during the approach (A–C) and on the retrace, an adhesion force pulls down on the tip until the point of detachment (D–F).

films was estimated from the analysis of four AFM height images of 5 μm × 5 μm obtained in tapping mode.

AFM Jumping mode was used to generate surface adhesion maps with a grid of 256 points × 256 points on a 5 μm × 5 μm area of the cast sample. In the AFM jumping mode, the tip-sample interaction is evaluated in each point by a normal force–distance curve (Fig. 1), where: (i) during the approach movement (A–C) the tip is pressed into the surface to a maximum indentation depth to finish the trace; and (ii) on the retrace movement (D–F), the sample is lowered away from the tip and an adhesion force pulls down on the tip. Then, an adhesion force maps was built from the maximum adhesion force measured in each surface points and the number of events (i.e., the number of points with a determined discretized values of forces) was plotted as a histogram.

Minimum film formation temperature (MFFT) of the synthesized latexes was determined employing an optical method [31]. It involved the observation of the clarity of a cast film (120 μm thickness) on a large metal table. A temperature gradient was applied to the table and the minimum temperature on it, where the film was judged to be clear, was considered as the MFFT value.

Differential scanning calorimetry (DSC) was performed using a TA Instrument Differential Scanning Calorimeter model Q2000. Casein showed a glass transition at 183 °C together with the beginning of its thermal decomposition. For this reason, DSC measurements of hybrid films were carried out from −80 to 130 °C at a heating rate of 10 °C/min. The sample (about 5 mg) was analyzed twice and the glass transition temperature (T_g) was determined as the temperature midpoint of the heat capacity change observed during the second run.

Moisture content of the films (MC) was determined by gravimetry. The MC was calculated as the relative weight difference in percentage after drying the film samples at 70 °C until constant weight. Film opacity was determined on rectangular strips directly placed on the UV–Visible spectrophotometer test cell. The absorption spectrum of the sample was obtained from 400 to 800 nm. Film opacity was defined as the area under the absorption spectrum of the sample obtained in the range 400–800 nm divided by the film thickness [32]. Measurements were taken by triplicate for each sample.

To evaluate the face-to-face blocking resistance of the films, latexes were applied on sealed paper (120 μm wet layer thickness) and dried during 48 h at room temperature. After drying, squares with an area of 38 mm × 38 mm were cut out of the sealed paper. The cut sections were placed with the film surfaces face-to-face for each sample to be tested and a pressure of 12.45 kPa was exerted on the specimens at a temperature of 60 °C to provoke blocking between both surfaces. The test was run at least three times and the results were correlated to rates on the scale of 0–10 (minimum and maximum blocking resistance, respectively) as defined by ASTM D 4946-89.

For the tensile tests, film specimens with dumbbell shape of length 9.53 mm and cross section 3.18 mm × 1 mm were cut. Tests were carried out in a TA HD plus Texture Analyzer equipment (Texture Technologies) at 23 °C, 50% relative humidity, and an elongation rate of 25 mm/min. At least five specimens of each sample were tested.

The hardness analysis was carried out with an universal testing machine (INSTRON 3344) with a 1000 N load cell, at 23 °C and 50% relative humidity. The indication of the hardness was measured as the maximum force in compression when a film is penetrated 1 mm with a 4 mm plane-cylinder probe. The surface of the sample was detected when a force of 0.05 N was measured.

Dynamic mechanical thermal analysis (DMTA) was used to analyze the relaxation behavior of the polymer–casein nanocomposites. To this effect, a film of 0.5 mm thick was presented in the single cantilever-bending mode at a frequency of 1 Hz between −80 and 150 °C at a heating rate of 4 °C/min, using a Tritec 2000 equipment of Triton Technology.

One important disadvantage of the acrylic films is the low resistant to organic solvents. For this reason the improvement of compatibility of acrylic–casein nanocomposites was evaluated by measuring the resistance to solvent immersion. For such analysis, film specimens of 20 mm in diameter were immersed in two different organic solvents, MEK (polar solvent) and Bz (non-polar solvent). Experiments were carried out at room temperature. Specimens were removed from the medium (MEK or Bz) at a regular time, dried with filter paper, and immediately weighed before immersing again. This procedure was repeated for 7 days or until the film presented damage. In each case, the relative mass absorbed (A_s) and the weight loss (WL_s), expressed as the percentage of the dissolved mass of the dried film, were calculated.

Soil burial degradation experiments were carried out to qualitatively determine the biodegradation ability of the hybrid films in composting condition. To this effect, specimens of 20 mm in diameter were buried in a vessel containing moisturized commercial compost with the following characteristics: total dry solid = 45% of the wet solids; non volatile-solids content = 40% of the wet solids; pH 6.5. Before the test, the compost was screened by a 3 1/2 mesh sieve (opening 5.6 mm). The test was run under controlled conditions of temperature (30 °C) and compost relative humidity of 55%. The samples were removed every 7 days, carefully cleaned in order to ensure the stop of the degradation and then dried in oven at 60 °C up to a constant weight. The weight loss rate (W_{loss}) of the film samples due to biodegradation was determined as the percentage of the mass lost from the initial film.

3. Results and discussion

3.1. Polymerization kinetics and molecular microstructure

Table 2 summarizes the results of experiments carried out with different amounts of casein and varied BA/MMA ratio, while maintaining constant the other reagents. The experiment codes contain the abbreviation C with a subscript that indicates the casein concentration in pphm, followed by the abbreviation MR with a subscript indicating the weight monomer ratio BA/MMA. Thus, in the experiment $C_3MR_{63/37}$, the casein concentration was 3 pphm and the weight BA/MMA ratio was 63/37.

In Table 2, the final values of x, d_p and CGE are presented, whereas Fig. 2a and b shows the evolution along the polymerizations of x, and CGE. When casein concentration was increased

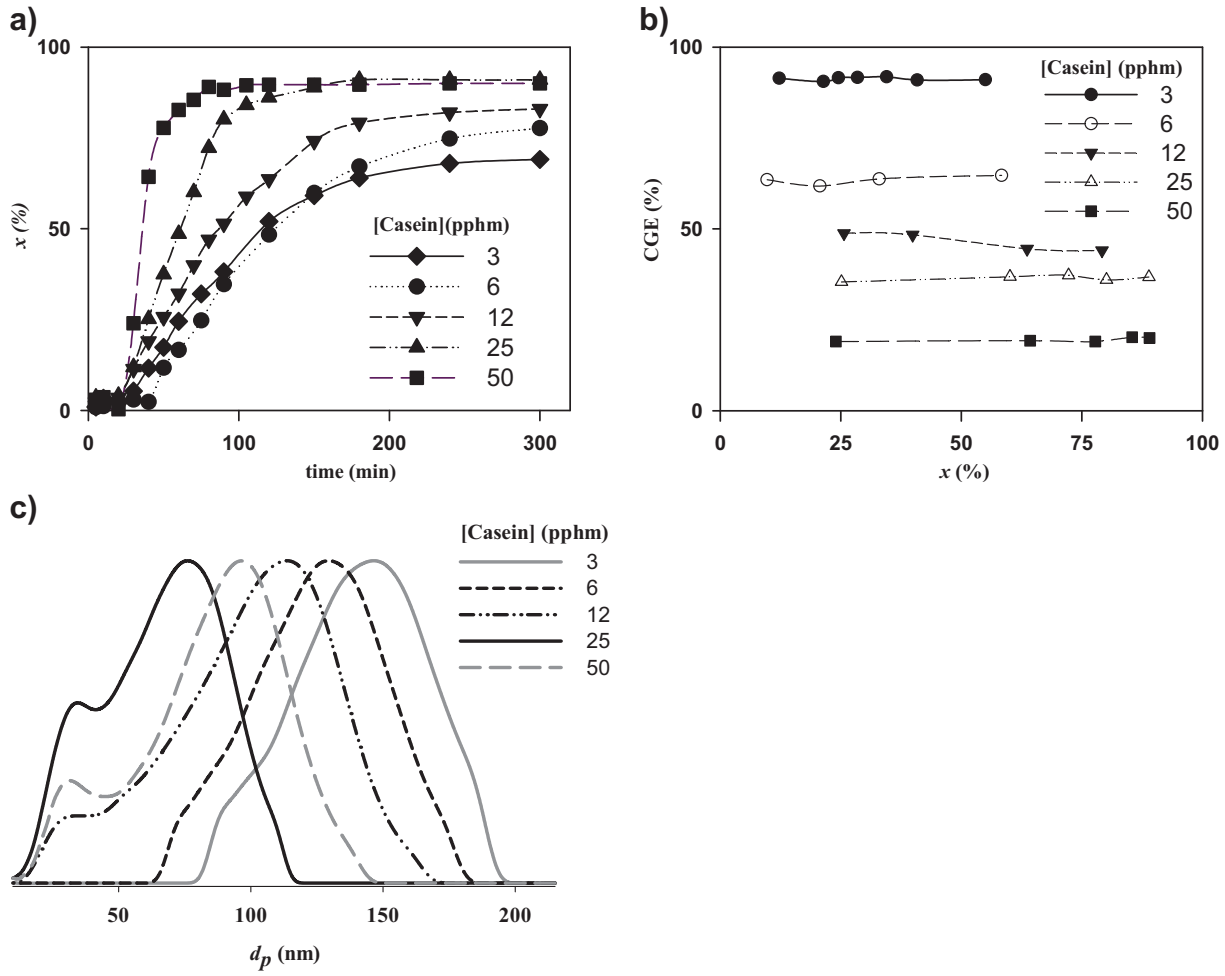

Fig. 2. BA/MMA emulsion polymerization in the presence of varied casein concentration. Evolution of: (a) conversion, and (b) CGE. (c) Final mass PSDs (distributions were normalized to the same maximum).

from 3 up to 50 pphm, higher values of both the initial polymerization rate, after a common induction period, and the final x were obtained. This behavior is in agreement with that observed for the MMA homopolymerization in the presence of varied casein concentration [28]. It was rather expected because the reaction is started by the presence of amino and tert-butoxy radicals, in turn produced by interaction of the hydroperoxide molecules with the amino groups present in the casein backbone [26]. Therefore, the larger the amount of casein, the greater the quantity of amino groups available for interacting with the TBHP.

When casein content increases, its grafted fraction decreases, and hence higher amount of free casein is present in the latex. The constant evolution of CGE of Fig. 2b along the polymerizations indicates that casein grafting occurs at the beginning of the process. Also, the PSD's of the final latexes with varied casein concentration show the presence of two particle populations (Fig. 2c), likely the compatibilized acrylic-graft-casein which are mainly formed at the beginning of the process, and the uncompatibilized particles, formed by acrylics stabilized by ungrafted protein. Similar observations were obtained from the MMA homopolymerization in the presence of casein [28].

Note that PSD's are shifted toward lower values of dp and particle size measured by DLS decreases when casein concentration was augmented from 3 to 25 pphm. This effect is due to the stabilization power of casein, which has a critical micellar concentration of 0.1 mg/ml [28] (5 times higher than the casein concentration used in $C_3MR_{63/37}$). The case with 50 pphm of casein is out of this tendency likely because the monomer formulation only contains BA; or in other words the MMA, with a higher water solubility than BA, was absent and less polymer particles could be homogeneously nucleated [28].

Table 2
BA/MMA polymerization in the presence of varied casein concentration (3–50 pphm). Main latex and molecular microstructure properties.

Experiment	x (%)	dp (nm)	CGE (%)[a]
$C_3MR_{63/37}$	69	194	91 (2.7)
$C_6MR_{65/35}$	78	166	63 (3.8)
$C_{12}MR_{70/30}$	83	154	44 (5.3)
$C_{25}MR_{80/20}$	91	122	24 (6.0)
$C_{50}MR_{100/0}$	90	154	10 (5.0)

[a] The weight of grafted casein per hundred grams of acrylic monomeris also reported between parenthesis.

3.2. Film morphology

The knowledge of the film morphology is essential to adequately understand the performance of the hybrid films, and for this reason a detailed study was carried out for films obtained from different casein concentrations. Fig. 3a–d shows AFM phase images of the films air interface with casein content of 3, 12, 25, and 50 pphm. The internal morphologies of the materials with 3 and 50 pphm of casein (minimum and maximum casein content studied) are also shown in Fig. 3e and f. For brevity, only phase images are presented

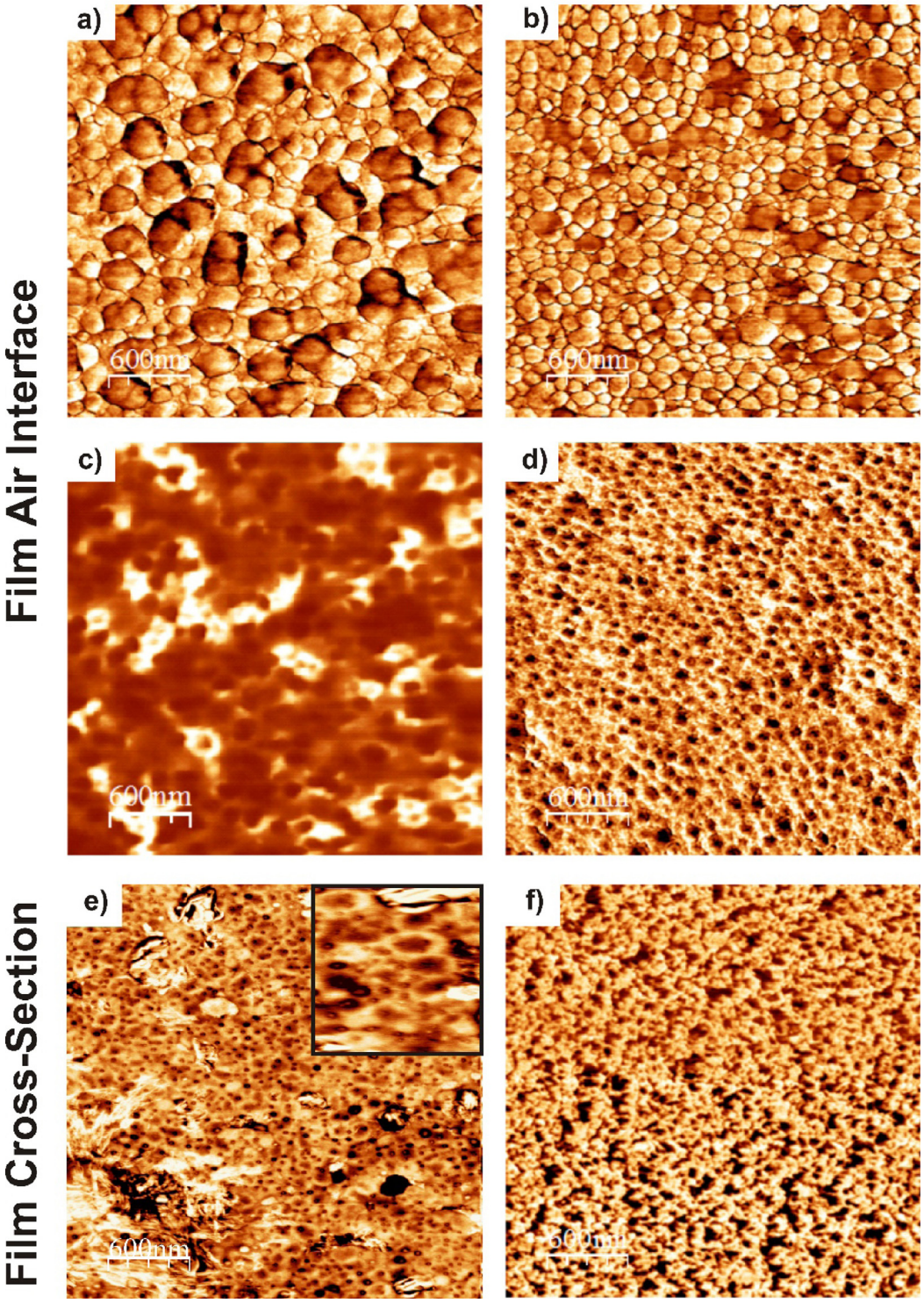

Fig. 3. AFM phase images (3.0 μm × 3.0 μm). Film surface (a–d) and cross-section (e and f) for casein concentrations of 3 pphm (a, e); 12 pphm (b); 25 pphm (c); and 50 pphm (d, f).

as they provide greater image contrast between the soft phase, that corresponds to the acrylic polymer (in dark color), and the hard domains of casein (in bright color).

When using low protein concentration (3–12 pphm), a high acrylic–casein compatibility was achieved (CGE = 91–44%), and hence casein is mostly grafted to the acrylic polymer. In this case, the phase images of the films surface are mainly constituted by the hard small domains of casein (Fig. 3a and b). The cross-section of the film $C_3MR_{63/37}$ (Fig. 3e, which also includes a zoom area of 0.5 μm × 0.5 μm) confirms the presence of partially coalesced core–shell particles, with a soft acrylic core and a thin hard-casein shell. This observation ratifies that the hard domains found in the film surface of samples with low protein contents correspond to the particles shell, mainly composed by grafted casein.

On the other hand, when high casein concentration were employed (25–50 pphm), the acrylic-biomaterial compatibility was significantly decreased (CGE = 24–10%), these latexes presenting a large amount of ungrafted casein. In this scenario, free casein acts

Fig. 4. Picture of films with different casein concentrations.

as a mobile phase and protein migration may occur during film formation, causing the generation of aggregates [33]. AFM phase image of the material with 25 pphm shows that the film surface is principally constituted by soft acrylic particles with some domains of hard casein (Fig. 3c), indicating that an appreciable fraction of ungrafted casein migrates toward the film bulk. When the protein content is even higher (50 pphm), a larger amount of ungrafted biomaterial is able to cover the film surface, forming a hard casein matrix with soft acrylic domains of small size (Fig. 3d). The distribution of the hard casein aggregates in the inner part of the film $C_{50}MR_{100/0}$ is similar to that observed on the film surface, where hard domains surrounds the soft acrylic particles (Fig. 3f).

It is worth pointing out that, phase segregation observed in films $C_{50}MR_{100/0}$ and $C_{25}MR_{80/20}$, was not present in films with lower casein concentration, which is an indication that the high percentage of grafted casein in those latexes avoided component migration during film formation.

3.3. Film properties

Table 3 summarizes the results of MFFT, MC, T_g, opacity and RMS roughness for the hybrid films together with those films of pure materials. In the code to pure films the subscript which indicates the concentration of the absent component is equal to 0. Despite casein is a hard material, with T_g close to 180 °C, the measured MFFT of casein solution was 11 °C, due to the high plasticization effect of water during the film formation process. The interaction of water with casein can be further supported by the MC of films containing casein, which is in all the cases higher than the pure acrylic film (see Table 3). MFFT of hybrid latexes resulted in all cases lower than 2 °C, which was the minimum temperature able to be measured with the equipment. Note that, despite formulations were adjusted to have similar T_g, the T_g of the hybrid polymers varied according to the monomer composition BA/MMA in the recipe, namely it was reduced as the BA content was increased. This is because, since phase separation in the graft copolymer was produced, two T_g's should be evidenced, one corresponding to the acrylic polymer and other one to the casein. However, casein showed a glass transition together with the beginning of its thermal decomposition, and for this reason, DSC measurements of hybrid films were carried out from −80 to 130 °C.

Optical properties are, to a great extent, relevant to the film application because of its impact on the film esthetic [34]. Hybrid latexes were able to form flexible and translucent films at room temperature (Fig. 4). While the film of pure casein is a bit opaque (opacity = 407 AU nm/mm), films of poly(BA-MMA) are more transparent (opacity = 160 AU nm/mm). Notice that the films opacity could be promoted by the surface and subsurface scattering of light and it depends on the casein content. The higher opacity observed in the film $C_3MR_{60/40}$ is a direct consequence of surface scattering due to its high roughness and of subsurface scattering from internal irregularities resulting from incomplete particle deformation and

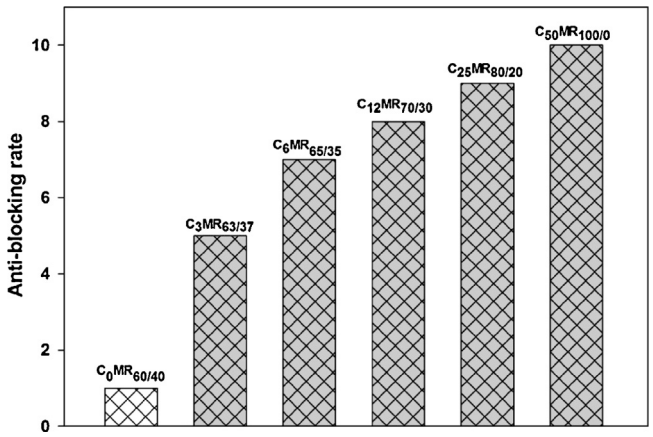

Fig. 5. Blocking resistance of hybrid acrylic–casein films with different casein concentration.

coalescence (Fig. 2e) [31,35]. The film roughness evolution shows that incorporation of casein promotes the formation of smoother films, considerably reducing the surface scattering. Also, casein aggregates observed by AFM in the film with higher casein content were much smaller than the visible wavelength, thus avoiding the subsurface scattering of visible light. For these reasons, opacity decreased as casein content was increased, resulting the films with high casein content (25–50 pphm) more transparent than the film of the acrylic homologous.

Block resistance is a key performance requirement for waterborne decorative coatings. As it is known, standard waterborne paints have poor block resistance. Fig. 5 shows that the incorporation of hard casein to soft acrylic formulations improves the blocking resistance, which is increased with the protein content. In the case of using 50 pphm of casein, a non-blocking film was obtained. This observation is in agreement with the improved block resistance observed when hard acrylic latexes were added to soft film forming latexes [10]. It is know that adhesion between two surfaces has both bulk and surface components. The addition of hard components to soft dispersions causes a hardening of the composite (thereby increasing the bulk storage modulus) and reduces the tack adhesion energy [36]. On the other hand, high effective concentration of hard components at the film surface also contributes to obtain greater anti-blocking performances.

Fig. 6a shows how the casein content reinforces the bulk film by increasing the shear storage modulus at temperature higher than 0 °C, and therefore a reduction in the tack adhesion energy with the casein content is expected. On the other hand, Fig. 6b compares the distribution of the measured adhesion force by AFM of the films surface of $C_{50}MR_{100/0}$, $C_{12}MR_{70/30}$, and $C_6MR_{65/35}$. These histograms confirm that adhesion force decreases with casein content (distributions are shifted toward lower values of adhesion force), which is consistent with the observed film morphology. At low protein contents, the film surface is mainly constituted by a thin shell of casein of soft acrylic cores from core–shell particles. This fine casein layer, principally composed by grafted casein (i.e., each protein molecule contains bounded at least one chain of soft acrylic), is not effective to reduce the adhesion force and completely prevent blocking. At high protein concentrations, the hard biomaterial is mainly ungrafted and hence has a high mobility. In such conditions, casein is able to form a fused percolated network (continuous hard/hard protein contact) on the film surface, which contributes to reduce blocking (or adhesion) [10]. It is worthy pointing out that, unlike the observed in hard and soft acrylic particles blends, the hard casein can fuse into a continuous percolated network at temperatures even lower than its T_g because of the water plasticization effect.

Table 3
Final values of MFFT, T_g, MC and opacity for the hybrid acrylic–casein and pure materials.

Experiment	MFFT (°C)	T_g (°C)	MC (%)	Opacity/thickness (AU nm/mm)	RMS roughness (nm)
$C_{100}MR_{0/0}$	11	183	11	407.3	12.4
$C_0MR_{60/40}$	<2	−12	0.4	160.6	40.3
$C_3MR_{63/37}$	<2	7	7	716.3	37.8
$C_6MR_{65/35}$	<2	−12	7	144.7	22.0
$C_{12}MR_{70/30}$	<2	−25	6	131.2	12.7
$C_{25}MR_{80/20}$	<2	−33	8	54.4	8.8
$C_{50}MR_{100/0}$	<2	−48	6	85.1	4.9

Table 4
Mechanical test results for hybrid acrylic–casein materials with different casein concentration.

Experiment	Tensile strength (MPa)	Elongation at break (%)	Hardness (N)
$C_{100}MR_{0/0}$	45.9 ± 5.9[37]	7.7 ± 0.8[37]	–[a]
$C_0MR_{60/40}$	5.1 ± 0.5	1213 ± 48	95.5 ± 9.7
$C_3MR_{63/37}$	3.1 ± 0.5	357 ± 63	54.3 ± 6.4
$C_6MR_{65/35}$	3.2 ± 0.3	720 ± 30	29.4 ± 4.2
$C_{12}MR_{70/30}$	2.4 ± 0.2	685 ± 21	344.9 ± 11.5
$C_{25}MR_{80/20}$	5.4 ± 0.3	370 ± 21	435.1 ± 22.2
$C_{50}MR_{100/0}$	6.7 ± 0.7	64 ± 2	1000 ± 0

[a] The pure casein films resulted too brittle for testing.

3.4. Mechanical behavior

Table 4 summarizes the mechanical test results of hybrid films together with those films from pure materials. At the test temperature (23 °C), pure BA/MMA copolymer is above their glass transition temperature (Table 3). Accordingly, it is in a rubber-like state and the deformation process is expected to occur by the existence of physical crosslinks (entanglements); as consequence very high deformations, without elastic recovery, were observed. The casein content in the hybrid films importantly affected their tensile behavior with respect to those of pure components. From Table 4 and Fig. 7, films with casein concentration lower than 50 pphm were able to support high deformations and presented increased toughness, while the sample with 50 pphm of casein broke at a low strain value. The observed behavior is related with the high concentration of ungrafted casein (90%), which is segregated inside the film. This segregated phase acts as a rigid nanofiller in the amorphous polymeric matrix, conferring a film performance similar to that of pure casein (small elongation at break and high tensile strength) [37]. Also, note that samples with high casein concentration (50–25 pphm) showed a clear yield zone at low strain (Fig. 7), which is an indication that the segregated ungrafted casein acts as a glassy component, conferring plastic characteristics to the films.

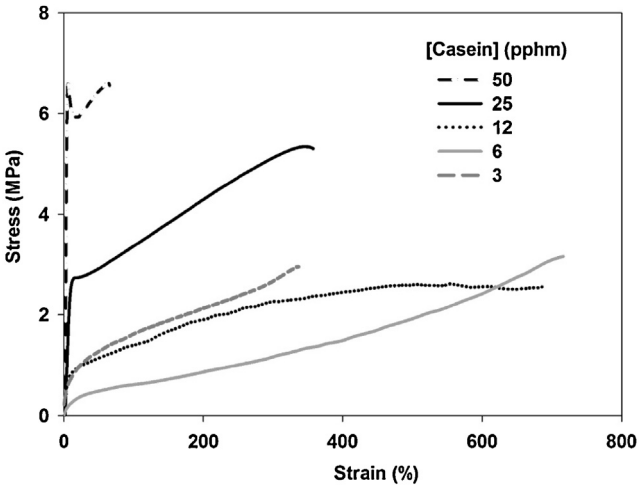

Fig. 7. Tensile test results for hybrid acrylic–casein films with varied casein concentration.

When casein concentration is lower than 25 pphm, phase separation is limited. Under these conditions, a synergetic behavior is observed. For example, samples containing 12 and 6 pphm of casein are elongated about 700% before failing. On the other hand, an early failure at 357% of elongation was observed in the sample with 3 pphm, probably due to the lower monomer conversion of this polymerization ($x < 70\%$), which became the composition of the acrylic polymer richer in the less flexible monomer, MMA.

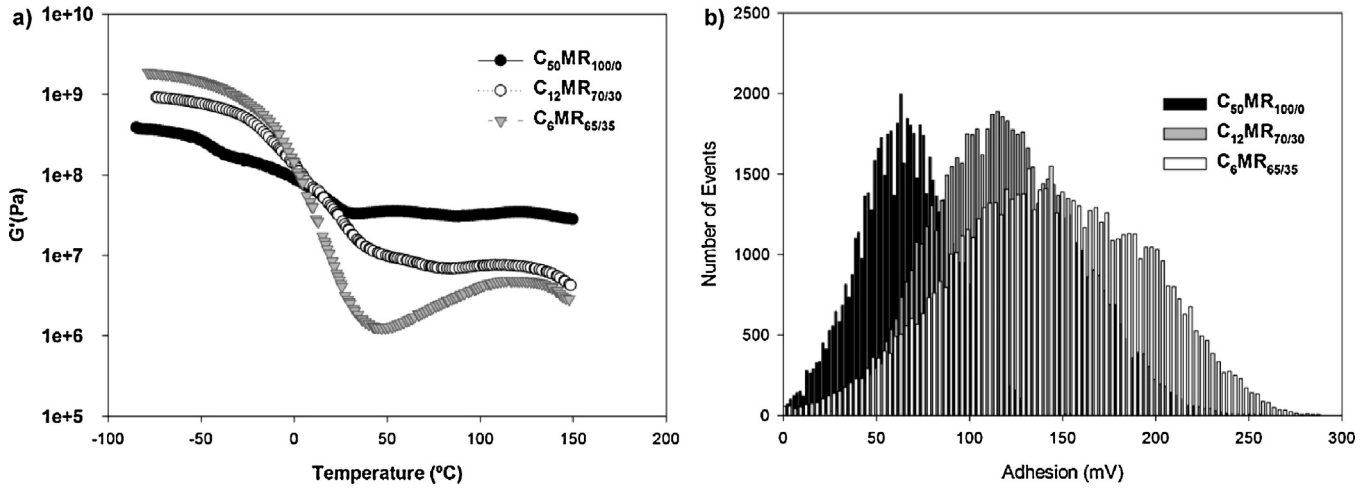

Fig. 6. Shear storage modulus, G' and the histogram of the measured adhesion force obtained by AFM adhesion mapping-force on films surface of $C_{50}MR_{100/0}$, $C_{12}MR_{70/30}$, and $C_6MR_{65/35}$.

Table 5
Solvent resistance for films with different casein concentration.

Experiment	A_s (%)		WL_s (%)	
	MEK	Bz	MEK	Bz
$C_{100}MR_{0/0}$	1.3	4.4	15.1	10.9
$C_0MR_{60/40}$	–	–	100.0	100.0
$C_3MR_{63/37}$	290.17	–	71.99	–
$C_6MR_{65/35}$	183.96	–	61.32	–
$C_{12}MR_{70/30}$	166.73	1016.39	36.74	41.12
$C_{25}MR_{80/20}$	70.63	956.94	23.84	24.04
$C_{50}MR_{100/0}$	29.31	475.15	14.02	15.11

One of the most important challenges in the coatings science is to simultaneously attain a good film forming and hardness. Acrylic polymers are good film-forming materials (they exhibit low MFFT, as shown in Table 3), but due to their low T_g, they present a poor hardness (Table 4). The incorporation of a hard component, as casein, to the soft acrylic polymer substantially increases the hybrid films hardness, as it can be seen from Table 4. When using 50 pphm of casein, the film hardness was notably improved, and was also observed that the higher the casein concentration the greater the increase in the film hardness.

From previous results, the incorporation of casein to the acrylic formulation largely fulfilled the requirement of film hardness and blocking properties, without affecting the film-forming capability of acrylic binders. On others words, some of the produced acrylic–casein hybrid latexes could be excellent alternatives as binder for waterborne coatings.

3.5. Solvent resistance

The solvent resistance results are summarized in Table 5. Measurements for pure casein showed that this material is almost unaffected by organic solvents; while the pure acrylic polymer is completely swollen in both MEK and Bz. Hybrid films showed increased solvent resistance with the protein content, since both the relative mass absorbed (A_s) and weight loss rate (WL_s) (for both solvents) decreased by increasing the casein content in the polymeric matrix. Higher swollen degrees are observed with Bz than with MEK, which could be attributed to the higher solvent power of the former. Samples with casein concentration of 3 and 6 pphm were disintegrated after 7 days of immersion in Bz, requiring a casein content higher than 6 pphm to resist immersion in this solvent.

On the basis of these results, it can be concluded that the presence of casein provides a sufficient barrier to organic solvent, evidencing a synergetic effect between both components.

Table 6
Soil biodegradation of the hybrid films.

Experiment	W_{loss} after 7 days (%)	W_{loss} after 14 days (%)
$C_{100}MR_{0/0}$	100[a]	100[a]
$C_0MR_{60/40}$	0.38	0.65
$C_3MR_{63/37}$	13.3	13.3
$C_6MR_{65/35}$	15.0	15.2
$C_{12}MR_{70/30}$	17.9	18.0
$C_{25}MR_{80/20}$	29.6	29.7
$C_{50}MR_{100/0}$	37.8	39.2

[a] The film lost their structural integrity and became attached to the soil after buried for 7 days. In this case, the sample was difficult to remove and weighed during the test.

3.6. Soil biodegradation

The results of soil biodegradation are presented in Table 6, as the weight lost by the films (W_{loss}) after 7 and 14 days. It is observed that the casein films lost their structural integrity and became attached to the soil after buried for 7 days, because it tends to hydrolyze and degrade easily under the action of microorganisms [24]. However, the acrylic polymer presented a very low degradation rate, which is an important drawback from the environmental point of view. Despite of the acrylic part was not degraded, the incorporation of casein improved the biodegradability of the materials, and the W_{loss} of the hybrid nanocomposites increased with the protein content.

4. Conclusions

Hybrid casein–acrylic dispersions containing different biomaterial contents were synthesized by emulsifier-free emulsion polymerization. The research was focused on the influence of the casein content and its degree of compatibility on the film properties. Due to the fact that the fraction of grafted casein was strongly dependent on the casein content of latexes, the film properties also showed a marked variation with its composition. Film morphology showed that when high casein content was used a large amount was non-grafted and segregated during the drying process. On the other hand, at low casein concentration the acrylic–casein compatibility was importantly enhanced, and therefore phase segregation during film formation was restricted. The incorporation of a component of high T_g as casein did not importantly affect the low MFFT and T_g of acrylic binders, which varied according to the BA/MMA ratio in the formulation, while improving their anti-blocking property, film hardness, resistance to organic solvent and soil degradability. Also, was observed that the films moisture content resulted independent of the casein concentration, discarding any influence of water content, on the films properties. In this way, it was demonstrated that the eco-friendly casein-based hybrid latexes satisfied the requirements for being used as binders in waterborne coatings.

Acknowledgements

The financial support received from CONICET, ANPCyT, the Secretary of Science, Technology and Research of Santa Fe State and the Secretary of University Policies from the Educational Ministry (all of Argentina) is gratefully acknowledged. We also acknowledge to the Physics of Surfaces and Interfaces Laboratory (IFIS Litoral, Santa Fe, Argentina) for the AFM characterizations.

References

[1] D. Urban, K. Takamura (Eds.), Polymer Dispersions and their Industrial Applications, Wiley-VCH Verlag GmbH & Co. KgaA, Weihein, 2002.
[2] G.W. Huber, S. Iborra, A. Corma, Chem. Rev. 106 (2006) 4044–4098.
[3] P. Li, J.H. Liu, Q. Wang, C. Wu, Macromol. Symp. 151 (2000) 605–610.
[4] H.K. Salzberg, L.E. Georgevits, R.M. Karapetoff Cobb, in: L.H. Silvernail, W.M. Bain (Eds.), Synthetic and Protein Adhesives for Paper Coating, Technical Association of the Pulp and Paper Industry, New York, 1961, pp. 103–166.
[5] S. Ednessjjad, in: S. Ednessjjad (Ed.), Adhesives Technology Handbook, William Andrew, Norwich, 2008, pp. 97–98.
[6] Y. Liu, Y. Zhang, Z. Liu, K. Deng, Eur. Polym. J. 25 (2002) 1619–1625.
[7] T.H. Kuan, US 43311738, 1982.
[8] S.S. Barry, US 5308890, 1994.
[9] M.A. Winnik, J. Feng, J. Coat. Technol. 68 (1996) 39–50.
[10] S.T. Eckersley, B.J. Helmer, J. Coat. Technol. 69 (1997) 97–107.
[11] A. Tzitzinou, J.L. Keddie, J.M. Geurts, A.C.I.A. Peters, R. Satguru, Macromolecules 33 (2000) 2695–2708.
[12] J.P. Tomba, D. Portinha, W.F. Schroeder, M.A. Winnik, W. Lau, Colloid Polym. Sci. 287 (2009) 367–378.
[13] S. Ugur, S. Sunay, O. Pekcan, Polym. Compos. 31 (2010) 1611–1619.
[14] J. Tang, V.L. Dimonie, E.S. Daniels, A. Klein, M.S. El-Aasser, Macromol. Symp. 155 (2000) 139–161.

[15] D. Colombini, H. Hassander, O.J. Karlsson, F.H.J. Maurer, J. Polym. Sci. Polym. Phys. 43 (2005) 2289–2306.
[16] J.S. Nunes, S.J. Bohórquez, M. Meeuwisse, D. Mestach, J.M. Asua, Prog. Org. Coat. 77 (2014) 1523–1530.
[17] D. Mohan, G. Radhakrishnan, T. Nagabhushanam, J. Appl. Polym. Sci. 25 (1980) 1799–1806.
[18] D. Mohan, G. Radhakrishnan, S. Rajadurai, J. Macromol. Sci. Chem. 20 (1983) 201–212.
[19] D. Mohan, G. Radhakrishnan, S. Rajadurai, J. Macromol. Sci. Chem. 22 (1985) 75–83.
[20] D. Mohan, G. Radhakrishnan, S. Rajadurai, Leather Sci. 33 (1986) 242–249.
[21] D. Mohan, G. Radhakrishnan, S. Rajadurai, J. Appl. Polym. Sci. 39 (1990) 1507–1518.
[22] J. Maldonado-Valderrama, A. Martin-Rodriguez, M.A. Cabrerizo-Vischez, M.J. Galvez Ruiz, in: R. Hidalgo-Álvarez (Ed.), Structure and Functional Properties of Colloidal Systems, Taylor and Francis Group, Norwich, 2010, pp. 219–233.
[23] Q. Xu, J. Ma, J. Zhou, Y. Wang, J. Zhang, Chem. Eng. J. 228 (2013) 281–289.
[24] J. Ma, Q. Xu, J. Zhou, D. Gao, J. Zhang, L. Chen, Prog. Org. Coat. 76 (2013) 1346–1355.
[25] X.H. Qiang, Q. Xue, H. Zhang, Z. Yan, M. Li, W. Xu, Y.J. Wang, J. Coat. Technol. Res. (2015), http://dx.doi.org/10.1007/s11998-014-9599-2
[26] P. Li, J. Zhu, P. Sunintaboon, F.W. Harris, Langmuir 18 (2002) 8641–8646.
[27] J. Zhu, P. Li, J. Polym. Sci. A: Polym. Chem. 41 (2003) 3346–3353.
[28] M.L. Picchio, R.J. Minari, V.D.G. González, M.C.G. Passegi, J.R. Vega, M.J. Barandiaran, L.M. Gugliotta, Macromol. Symp. 344 (2014) 76–85.
[29] Y. Liu, R. Gou, Biophys. Chem. 136 (2008) 67–73.
[30] I. Horcas, R. Fernández, J.M. Gómez-Rodríguez, J. Colchero, J. Gómez-Herrero, A.M. Baro, Rev. Sci. Instrum. 78 (2007) 013705.
[31] J.L. Keddie, Mater. Sci. Eng. 21 (1997) 10l–170l.
[32] J. Irissin-Mangata, G. Baudin, B. Boutevin, N. Gontard, Eur. Polym. J. 37 (2001) 1533–1541.
[33] M. Goikoetxea, Y. Reyes, C.M. de las Heras Alarcón, R.J. Minari, I. Beristain, M. Paulis, M.J. Barandiaran, J.L. Keddie, J.M. Asua, Polymer 53 (2012) 1098–1108.
[34] S. Mali, M.V.E. Grossmann, M.N. Martino, N.E. Zaritzky, Carbohydr. Polym. 56 (2004) 129–135.
[35] F.M. Monedero, M.J. Fabra, P. Talens, A. Chiralt, J. Food Eng. 91 (2009) 509–515.
[36] R.S. Gurney, D. Dupin, J.S. Nunes, K. Ouzineb, E. Siband, J.M. Asua, S.P. Armes, J.L. Keddie, Appl. Mater. Interfaces 4 (2012) 5442–5452.
[37] N. Somanathan, M.D. Naresh, V. Arumugam, T.S. Ranganathan, R. Sanjeevi, Polym. J. 24 (1992) 603–6011.